



**Acoustics'08
Paris**
June 29-July 4, 2008
www.acoustics08-paris.org

A review of the scattering properties of suspended sandy sediments for the application of acoustics to sediment transport studies

Peter Thorne^a and Ramazan Meral^b

^aProudman Oceanographic Laboratory, Joseph Proudman Building, 6, Brownlow Street, L3 5DA Liverpool, UK

^bKahramanmaras Sutcu Imam University, Faculty of Agriculture, Department of Agricultural, Structures and Irrigation, 46060 Kahramanmaras, Turkey
pdt@pol.ac.uk

Multi-frequency acoustics backscattering has been used for over a decade, to quantitatively measure, in the marine environment, near-bed profiles of suspended sediment particle size and concentration. Central to obtaining the sediment parameters from the backscattered signal, is a description of the scattering properties of irregularly shaped particles randomly distributed in space. Formulations are therefore required for both the attenuation and backscattering properties of suspensions of sedimentary particles with size and acoustic frequency. There is no rigorous analytical solution or single formulation for these scattering properties and different researchers have used somewhat different expressions. Here we bring together four decades of published data on the acoustic scattering properties of suspensions of sandy sediments. These data are reformulated in terms of the usual acoustic scattering nomenclature, that is the form function and the normalised total scattering cross-section and simple heuristic generic expressions, based on a sphere scattering model, are formulated to describe the sediment scattering properties. The expressions are not limited to sand particles, but should have broad applicability to irregularly shaped particle scattering.

1 Introduction

Here we highlight the use of multi-frequency acoustic backscattering systems, ABS, for measuring suspended sediments over sandy beds. The multi-frequency ABS's currently in use typically operate in transceiver mode, usually at frequencies in the range 0.5 MHz – 5MHz [1-2]. The aim is to use the differential scattering characteristics of the scatterers with frequency to establish the suspended sediment particle size and concentration. Because ABS's are normally used in transceiver mode, it is the backscattering and attenuating characteristics of the suspended sediment which are required for converting the acoustic measurements into suspended sediment parameters. The relevant acoustic quantities are the backscatter form function, f , which describes the backscattering characteristics of the particles in suspension, and the normalized total scattering cross-section, χ , which describes the attenuating characteristics.

The sphere scattering approach, using the f and χ representation, was first adopted by Sheng and Hay [3] to explain the sediment attenuation observations of Flammer [4]. They used a rigid mobile sphere model which compared reasonably well with the measurements and they also formulated a simple heuristic expression which also provided good agreement with the data. Other publications [5-11] have adopted a similar approach and presented similar, though different expressions, related to particular data sets. In this study the objective was to bring together the published literature on acoustic scattering by suspensions of sandy sediments and irregularly shaped particles. The aim was to provide simple expressions for f and χ which compared well with all the data sets available and which can be used with a reasonable degree of confidence in the interpretation of ABS data collected above sandy sediments.

2 Suspension scattering

The backscattered signal from a multi-frequency ABS can be converted to concentration, M , and mean particle size, $\langle a \rangle$, using (1,3,6,8,11).

$$M = \left\{ \frac{V_{rms} \psi r}{k_s k_t} \right\}^2 e^{4r(\alpha_w + \alpha_s)} \quad (1)$$

$$k_s = \frac{\langle f \rangle}{\sqrt{\langle a \rangle \rho}}, \quad \alpha_s = \frac{3}{4r\rho} \int_0^r \frac{\langle \chi \rangle M}{\langle a \rangle} dr$$

The above expression assumes the attenuation over a range bin is not substantial [11]. V_{rms} is the root-mean-square backscattered signal; this is an ensemble average over a number of backscatter returns. r is the range from the transceiver, ψ accounts for the departure from spherical spreading within the transducer nearfield, k_s and α_s represent respectively the backscattering and attenuating properties of the sediments, ρ is the density of the sand grains in suspension, k_t is a system constant [12], α_w is the attenuation due to water absorption and the other terms are given below.

$$\langle a \rangle = \int_0^\infty a P(a) da \quad (2)$$

$$\langle f(x_o) \rangle = \left\{ \frac{\int_0^\infty a P(a) da \int_0^\infty a^2 f(x)^2 P(a) da}{\int_0^\infty a^3 P(a) da} \right\}^{1/2} \quad (3)$$

$$\langle \chi(x_o) \rangle = \frac{\int_0^\infty a P(a) da \int_0^\infty a^2 \chi(x) P(a) da}{\int_0^\infty a^3 P(a) da} \quad (4)$$

Where a is the radii of the sediment grains in suspension, $P(a)$ is the probability size distribution of the grains and $x=ka$, where k is the wave number of the sound in water and $x_o=k\langle a \rangle$. The variable x is non-dimensional and as will be seen below is an appropriate choice for describing the dependency of f and χ . As a step towards the evaluation of equation (1), equations (3) and (4) need to be calculated and this requires expressions for f and χ . The purpose of the present paper is to provide these expressions using all the presently available published data, so that marine scientists can use them in a straightforward manner in the interpretation of ABS data.

Although there is no general analytical solution to the scattering properties of irregularly shaped particles some reasonable estimates can be made for $x \ll 1$ and $x \gg 1$. For $x \ll 1$, the Rayleigh regime, the wavelength of the sound is much greater than the particle circumference and scattering is considered to be independent of the shape of the scatterer. Therefore one might anticipate spherical and irregularly shaped scatterers may have similar scattering

characteristics. Rayleigh scattering for a sphere is given by [13].

$$f = 2x^2 \left[\frac{e-1}{3e} + \frac{g-1}{2g+1} \right] \quad (5a)$$

$$\chi = 2x^4 \left[\left(\frac{e-1}{3e} \right)^2 + \frac{1}{3} \left(\frac{g-1}{2g+1} \right)^2 \right] \quad (5b)$$

$e=E_1/E_0$ is the ratio of elasticity of sand grains (quartz) to water, $e=39$, and g is the ratio of the density of the sand grains to water, $g=2.65$. Putting the values for e and g into equation (5) gives $f=1.17x^2$ and $\chi=0.26x^4$; these are particularly simple expressions. For $x \gg 1$, the geometric regime, the scattering cross-section is the particle's actual cross-section. There is a theorem [14,15] that states that the geometric cross-section of a convex particle, averaged over all orientations, is equal to a quarter of the surface area of the particle. Since a sphere has the minimum surface area to volume, then it is expected that a particle of irregular shape, having a similar volume to a sphere, would have a larger surface area and hence a higher geometric and scattering cross-section. For a rigid sphere f and χ tend to a constant value of unity for $x \gg 1$ and therefore it might be reasonable to anticipate that for irregularly shaped particles f and χ would tend to a constant value somewhat greater than unity.

3 Measurement and formulations

The first quantitative suspended sediment measurements which were expressed in the form function formulation were collected on beach sands [11]. Acoustic backscatter measurements from a sediment jet were collected at 1.0 MHz, 2.25 MHz and 5.0 MHz, using three beach sands sieved into $\frac{1}{4}\phi$ size intervals and covering the radius range 58-231 μm . Following on from these measurements, broadband scattering from the sediment jet were carried [16]. Data were collected on $\frac{1}{4}\phi$ sieved sand samples with mean radii of 57.75 μm , 98.0 μm and 162.5 μm , over the concentration range 0.35-5.66 kgm^{-3} and covering the frequency band 1.25-2.75 MHz in 0.2 MHz frequency intervals. Further measurements were reported [9] using sands collected from estuarine, beach and quarried locations. Observations were made in a sediment tower which generated a homogeneous suspension of sediments over a vertical range of about 1m. Data were collected over the particle radius range 45-390 μm in $\frac{1}{4}\phi$ sieved intervals. The acoustic frequencies used were 1.0 MHz, 2.0 MHz and 4.0 MHz. Finally a series of measurements have been published on scattering by single irregularly shaped particles [17]. Measurements were collected on particles in the radius range 0.72-2.5 cm using a broadband system operating between 40-240 kHz and on particles with radius between 0.15-0.2 cm using narrow band signals over the frequency range 0.6-2.2MHz.

The earliest useful published measurements on attenuation by suspensions of sandy sediments were reported over forty years ago [4]. These data were used [3] to provide the first contemporary description of suspended sediment attenuation using sphere scattering models and a simple 'high-pass' heuristic model, which provided good

agreement with the observations. The measurements were collected over the radius range 26-455 μm , at six discrete frequencies between 2.5-25.0 MHz at a fixed concentration of 2.65 kgm^{-3} . Sheng and Hay [3], in their table 2, also presented attenuation data from other studies [18-20], which we have also included here. The next data set is from the suspended sediment jet work [11]. Measurements were made over a range of concentrations nominally between 0.3-24 kgm^{-3} , using a selection of beach sands sieved into $\frac{1}{4}\phi$ size intervals, at frequencies of 2.25 MHz, 4.5 MHz and 5.0 MHz. Both a rigid sphere model with the density of quartz and the high-pass model were compared with the data. More recent [7] attenuation measurements were made on sandy sediments over the frequency range 2.25-100 MHz using $\frac{1}{4}\phi$ sieved radii of 11.5 μm , 24.5 μm , 49 μm and 98 μm . Lastly, attenuation measurements were obtained from the gradient of the backscattered signal as part of the sediment tower study [9].

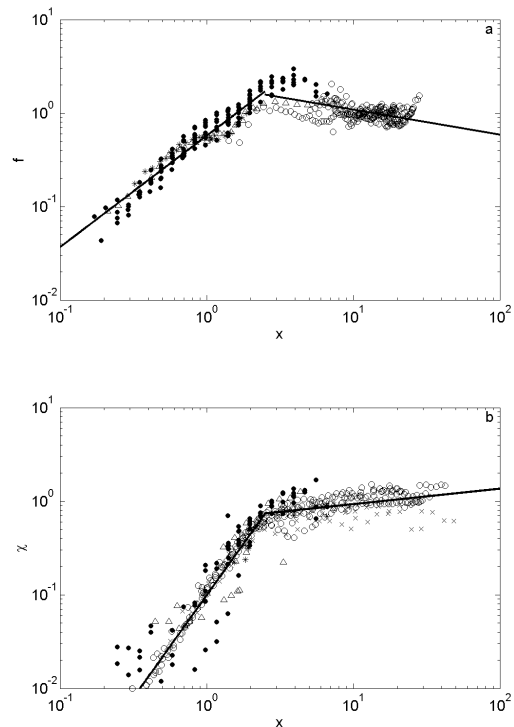


Fig. 1. a) Measurements of the form function, f , from; [11] (Δ), [16] ($*$), [17] (\circ) and [9] (\bullet). b) Measurements of the normalized total scattering cross-section, χ , from; [4] (x), [3] ($*$) (using the data [18-20]), [11] (Δ), [7] (\circ) and [9] (\bullet). The solid lines are linear regression fits to the logarithm of the data for $x \leq 2.5$ and $x > 2.5$.

The data from the four studies on the form function for sandy suspensions and irregularly shaped particles are shown in figure 1a. The data cover the range $x=0.2-30$. In general the observations are similar in form for the different data sets; this is indicative that the non-dimensional scattering parameters used on the abscissa and the ordinate are appropriate for scattering by irregularly shaped particles. There is scatter in the data and this is considered to be associated with detailed differences in particle shape [7], different experimental procedures and experimental errors associated with the different data sets. As can be seen in

figure 1a, between $x=0.2-2$ there is seen to be a relatively steady increase in the form function with x and with the trend being nominally consistent for the different data sets. Above the value of $x \approx 2$, the increase of f with x is no longer dominant and the data show somewhat less consistency. Above $x \approx 5$, the data available is only for single irregularly shaped scatters and the trend is nominally uniform with a possible slight reduction in form function as x increases. The complementary results for the measurements of the normalized total scattering cross-section are presented in figure 1b. Data were obtained between $x=0.3-50$. Again, as with the form function, the different data sets of the normalized total scattering cross-section generally follow a similar trend. The data show increasing values for χ with x up to a value of $x \approx 2$ and with a gradient steeper than was the case for the form function. Above $x \approx 2$ the rate of increase of χ with x is significantly reduced and at higher values of x , $x > 10$, χ appears to be nominally independent of x .

Plotted in figures 1a and 1b are linear regressions carried out on the logarithm of the data, for $x \leq 2.5$ and $x > 2.5$. The value of $x=2.5$ was chosen as the break point in the regression fitting because of the change in gradient at approximately this value of x . The regression lines were not fitted as theoretical matches to the data, but simply as a way of removing outliers from the general trends in the data. Data lying at a significant distance from the lines was considered as outside the general trends in the data. Figure 2 shows ratios of the measured values for f and χ divided by the calculated values from the linear regression fit to the data, f_r and χ_r . Values of this ratio between $1.5^{-1}-1.5$ were deemed as acceptable data. These boundaries retained most of the measurements, 92% for f , 81% for χ , while removing measurements which were outside the general body of the data sets.

Using the data within the $1.5^{-1}-1.5$ specified boundaries; an averaging process was used to reduce the scatter in the data. Data between $x=0.1-1$ were averaged over $x \pm 0.01$ intervals, data in the range $x=1-5$ were average over $x \pm 0.1$ intervals, data in the range $x=5-20$ were averaged into $x \pm 0.5$ intervals and above $x=20$ data were averaged into $x \pm 1$ intervals. These averaging intervals retained the form of the data and clarified the trends. The results are shown in figure 3, with error bars, derived by calculating the standard deviation of the f and χ values over the averaging intervals of x . Compared with figure 1 the trends in the data are somewhat clearer. In figure 3a the values for f steadily increase with x until $x \approx 1$, between $x=1-2$ there seems to be a region of inflexion in the data, between $x=2-4$ there is some variability in the data and above $x=10$ the form function is nominally constant in value. In figure 3b the values for χ are seen to increase rapidly with x up to $x \approx 2$, the gradient of the data then decreases with x , with χ becoming nominally independent of x for $x > 10$.

To represent the measurements, formulae were derived on a heuristic basis and following procedures presented in previous publications [1,3,6,8]. Asymptotic constraints were imposed such that for $x \ll 1$, the Rayleigh regime, $f \propto x^2$ and $\chi \propto x^4$ and for $x \gg 1$, the geometric regime, f and χ were constant. For the form function the expression used was

$$f = \frac{x^2 \left(1 - \varphi_1 e^{-((x-x_1)/\zeta_1)^2} \right) \left(1 + \varphi_2 e^{-((x-x_2)/\zeta_2)^2} \right)}{1 + \delta_1 x^2} \quad (6)$$

For $x \ll 1$, the two bracketed terms tend to a constant, c_0 , hence $f = c_0 x^2$. For $x \gg 1$, $f = 1/\delta_1$ which is constant and independent of x . The first bracket containing the

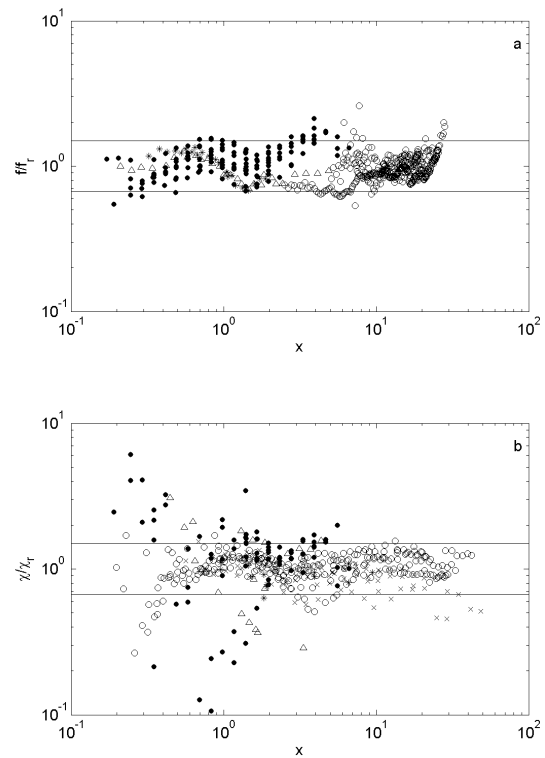


Fig. 2. a) Plot of the ratio of the measured form function, f , to the form function calculated from the regression lines in figure 1a, f_r . b) Plot of the ratio of the measured normalized total scattering cross-section, χ , to the normalized total scattering cross-section calculated from the regression lines in figure 1b, χ_r . The two horizontal lines represent ratios equal to 1.5^{-1} and 1.5 . The symbols used in figure 2 correspond with those used in figure 1 and their associated data sets.

exponential introduces the inflexion region around $x=1-2$. Physically this is associated with a back and forth movement of the particles in the water due to the propagating acoustic wave. The second bracket accounts for the observed peak in the form function at approximately $x=2-4$, before the onset of the expected constant value for f at the higher values of x . The bracketed terms have six independent variables and these were obtained by matching the predictions to the data in the local area where the bracketed terms have maximum influence and then by fine tuning equation (6) to minimizing the mean root-mean-square difference between the predictions and the data. The result was

$$f_e = \frac{x^2 \left(1 - 0.35 e^{-((x-1.5)/0.7)^2} \right) \left(1 + 0.5 e^{-((x-1.8)/2.2)^2} \right)}{1 + 0.9 x^2} \quad (7)$$

This simple expression, given by the solid line in figure 3a, captures the essential features of the data; Rayleigh scattering for $x \ll 1$, the curvature of the data in the region $x=1-5$ and constant in the geometric scattering regime. For small values of x , $f_e = c_0 x^2$, where $c_0 = 1.25$, this value is comparable, though slightly higher, 7%, than the predicted

value from equation (5a). For large x , $f_e=1.1$. Asymptotic expressions for $x \ll 1$, $f_e=1.25x^2$ and $x \gg 1$, $f_e=1.1$, are respectively given by the dashed and dotted lines in figure 3a.

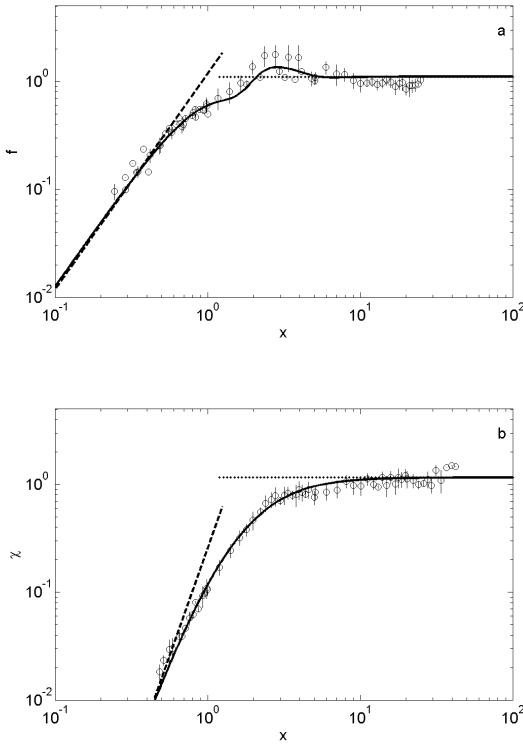


Fig. 3. a) Measurements of the filtered and smoothed form function (o), equation (7) (—), Rayleigh scattering (---) and geometric scattering (···). b) Measurements of the filtered and smoothed normalized total scattering cross-section (o), equation (9) (—), Rayleigh scattering (---) and geometric scattering (···).

For the normalized total scattering cross-section the expression below was used, this is similar to the expression used in Ref [3].

$$\chi = \frac{\beta_1 x^4}{[\xi_1 + \xi_2 x^\kappa + \beta_2 x^4]} \quad (8)$$

Following the approach taken with the form function, for $x \ll 1$, $\chi = (\beta_1/\xi_1)x^4$ and β_1/ξ_1 was obtained from the low x values. For $x \gg 1$, $\chi = \beta_1/\beta_2$, this was obtained from the data. ξ_1 , ξ_2 and κ were then adjusted to minimize the root-mean-square difference between equation (8) and the measurements. The result was

$$\chi_e = \frac{0.29x^4}{[0.95 + 1.28x^2 + 0.25x^4]} \quad (9)$$

As shown in figure 3b, the solid line obtained using equation (9) represents all the main features of the data, with close agreement in the Rayleigh, intermediate and geometric regimes. For $x \ll 1$, $\chi_e = 0.3x^4$, this is marginally higher than predicted using equation 5(b) by 11%, which is similar to the 7% for the form function in the Rayleigh regime. For $x \gg 1$, $\chi_e = 1.16$, this is comparable with the value for the form function in the geometric scattering

regime. $\chi_e = 0.3x^4$ and $\chi_e = 1.16$ are respectively shown by the dashed and dotted lines in figure 3b.

4 Conclusion

The present work has sought to provide scattering expressions, for the interpretation of data collected using multi-frequency acoustic backscatter systems, in the study of near bed small-scale sediment transport studies over sandy beds. The use of acoustics for such studies has gained increasing acceptance by sedimentologists and coastal engineers over the past decade or more. To obtain profiles of suspended sediment concentration and particle size, from the backscatter data, requires a description of the acoustic scattering properties of the sediments in suspension. As noted in the text different researchers have used somewhat different expressions to represent the backscattering and attenuating properties of suspensions of sandy sediments. All the expressions are based on sphere scattering, and it is from this acoustic sphere scattering literature, that the definition and nomenclature of using the form function to describe the backscattering characteristics and the normalized total scattering cross-section to represent the attenuation is derived. Because there are no readily available analytical solutions to the scattering by randomly shaped particles, understanding the scattering of suspensions of sand grains has advanced by experimental observation, modifications to the model of sphere scattering and by the use of simple heuristic expressions.

To obtain simple formulation for the scattering properties, all the published data available on scattering by suspensions of sandy sediments were collated. These data have also been augmented by some measurements taken on single irregularly shaped particles. All the data sets were formulated in terms of the form function and normalized total scattering cross-section, so that the results could be directly applied to the interpretation of acoustic backscatter data. The combined data sets had a degree of scatter, and therefore before fitting expressions to the data outliers were identified and rejected. This was followed by smoothing over narrow ranges of x , which highlighted the main features in the data. Simple heuristic expressions, in the form of equations (6) and (8) were put forward which encompassed Rayleigh scattering for $x \ll 1$, and geometric scattering for $x \gg 1$. Using the measurements in the Rayleigh and geometric scattering regimes, some of the constants in the expressions were established. Other constants were obtained by minimizing the root-mean-square difference between the predictions and the observations. This led to the expressions given in equations (7) and (9). Other formulations for f_e and χ_e were assessed using a regression approach and the expressions of Crawford and Hay [1] and Thorne and Hanes [8] were only marginally poorer predictors than those presented here, although the former does not conform to Rayleigh scattering when $x \ll 1$.

Finally, the aim of the present paper has been to provide those who use acoustics as a tool for studying sediment transport processes, with simple expressions for the scattering properties of suspensions of sandy sediments. Equations (7) and (9) represent a best fit to the published data available at present, with the constraint of Rayleigh scattering for $x \ll 1$ and geometric scattering for $x \gg 1$.

These equations, in conjunction with equation (3) and (4), provide a simple basis for interpreting data obtained using multi-frequency ABS over sandy seabeds.

Acknowledgments

This work was supported by NERC UK as part of its small scale sediment process studies. PDT would like to thank ONR USA which partially supported this work under its mine burial programme. RM was supported by Kahramanmaraş University and the Proudman Oceanographic Laboratory during his visit to the Proudman Oceanographic Laboratory in 2006. This work was first published in *Continental Shelf Research* in 2008 [10].

References

- [1] A. M. Crawford and A. E. Hay, "Determining suspended sand size and concentration from multifrequency acoustic backscatter", *J. Acoust. Soc. Am.* 94(6), 3312-3324 (1993)
- [2] P. D. Thorne, J. J. Williams and A. G. Davies, "Suspended sediments under waves measured in a large scale flume facility", *J. Geophysical Research*. Vol 107, No C8, 10.1029/2001JC000988. 4.1-4.16 (2002)
- [3] J. Sheng and A.E. Hay, "An examination of the spherical scatterer approximation in aqueous suspensions of sand", *J. Acoust. Soc. Am.* 83, 598-610 (1988)
- [4] G. H. Flammer, "Ultrasonic measurements of suspended sediments", *Geological Survey Bulletin No 1141-A*, United States Government Printing Office, Washington (1962)
- [5] A. E. Hay and J Sheng, "Vertical profiles of suspended sand concentration and size from multifrequency acoustic backscatter", *J. Geophys. Res.* 97(C10). 15661-15677 (1992)
- [6] P. D. Thorne, P. J. Hardcastle, R. L. and Soulsby, "Analysis of acoustic measurements of suspended sediments", *J. of Geophysical Res.*, Vol. 98, No. C1, 899-910 (1993)
- [7] A. S. Schaafsma A. S. and A. E. Hay, "Attenuation in suspensions of irregularly shaped sediment particles: A two-parameter equivalent spherical scatterer model", *J. Acoust. Soc. Am.* 102, 1485-1502 (1997)
- [8] P. D. Thorne P.D. and D. M. Hanes, "A review of acoustic measurement of small scale sediment processes", *Continental Shelf Res.* 22, 603-632 (2002)
- [9] P. D. Thorne and M. J. Buckingham, "Measurements of scattering by suspensions of irregularly shaped sand particles and comparison with a single parameter modified sphere model", *J. Acoust Soc Amer.* 116 (5) 2876-2889 (2004)
- [10] P. D Thorne and R Meral, "Formulations for the scattering properties of sandy sediments for use in the application of acoustics to sediment transport", *Continental Shelf Research*, 28, 309-317 (2008)
- [11] A. E. Hay, "Sound scattering from a particle-laden turbulent jet", *J. Acoust Soc. Am.*, 90, 2055-2074 (1991)
- [12] K.F.E. Betteridge, P.D. Thorne and R. D. Cooke, "Calibrating multi-frequency acoustic backscatter systems for studying near-bed suspended sediment transport processes", *Continental Shelf Research*, 28, 227-235 (2008)
- [13] C.S. Clay and H. Medwin, "Acoustical Oceanography: Principles and applications", Published by John Wiley & Sons USA (1997)
- [14] H C van de Hulst, "Light scattering by small particles", New York, Dover Publications. pp470 (1981)
- [15] P. A. Chinnery, V. F. Humphrey and J. Zhang, "Low-frequency acoustic scattering by a cube. Experimental measurements and theoretical predictions" *J. Acoust Soc Amer.* 101, 2571-2582 (1997)
- [16] C. He and A. E. Hay, "Broadband measurements of the acoustic scattering cross section of sand particles in suspension", *J. Acoust. Soc. Am.* 94(4) 2247-2254 (1993)
- [17] P. D. Thorne, K. R. Waters and T. J. Brudner, "Acoustic measurements of scattering by objects of irregular shape", *J. Acoust. Soc. of Am.*, 97(1), 242-251 (1995)
- [18] R. H. J Jansen, "The in-situ measurement of sediment transport by means of ultrasound scattering. A Delft Hydraulics Laboratory report", The Netherlands, publication number 203, pp13 (1978)
- [19] R. H. J. Jansen, "An Ultrasonic Doppler Scatterometer for Measuring Suspended Sand Transport", in *Ultrasonic International 79*, Conference Proceedings, edited by Z. Novak (Graz, Austria), UI 79, 366-371 (1979)
- [20] A. S. Schaafsma and W. J. G. J. der Kinderen, "Ultrasonic instruments for the continuous measurement of suspended sand transport", *Proceedings of the IHAR symposium on Measuring Techniques in Hydraulic Research* (editor A.C.E Wessels) held at Delft Hydraulics 22-24 April 1985 and published by A. A. Balkema Rotterdam in 1986. 125-136 (1985)